IEICE TRANSACTIONS

on Fundamentals of Electronics, Communications and Computer Sciences

DOI:10.1587/transfun.2024EAP1089

Publicized:2024/12/06

This advance publication article will be replaced by the finalized version after proofreading.

A PUBLICATION OF THE ENGINEERING SCIENCES SOCIETY

The Institute of Electronics, Information and Communication Engineers

Kikai-Shinko-Kaikan Bldg., 5-8, Shibakoen 3 chome, Minato-ku, TOKYO, 105-0011 JAPAN

PAPER

Analysis of series-connected double-layer coils for MHz inductive power transfer

Quang-Thang DUONG[†a)], ***Member***, **Kohei MATSUKAWA**[††], **Quoc-Trinh VO**[††], ***Nonmembers***, ***and*** **Minoru OKADA**[†††], ***Member***

SUMMARY Double-layer coils (DLCs) have been extensively investigated for compact inductive power transfer (IPT) systems operating in the MHz frequency range. Different from previous studies which focus mainly on realizing self-resonance and enhancing the Q factor, this paper enhances both the Q factor and the self inductance to achieve high efficiency and guarantee target output voltage when deployed in IPT applications. By using a lumped-element model derived from transmission line concept, this paper shows that the self inductance when the two layers are serially connected is approximately more than 3 times of that when the two layers are open-ended. Motivated by this feature, we focus on the series-connected DLC and investigate a resonance scheme using two external capacitors: one inserted between the two layers and the other inserted outside the coil. In this resonance scheme, parameters of the capacitors are chosen not only to enhance the Q factor but also to maintain the self inductance. Our air-cored sample coils of 100 mm outer diameter exhibit self inductance of 7.69 μH, Q of 308 at 6.78 MHz, and 94% power transfer efficiency at 50 mm transmission distance. These results are attractive when compared to recent self-resonant open-ended DLCs having similar dimensions.

key words: *Double-layer coil, Q factor, inductance, efficiency.*

1. Introduction

Inductive power transfer (IPT) [1], [2] is a non-radiative type of wireless energy transmission which couples alternating current (AC) from the primary coil to the secondary coil by utilizing electromagnetic induction. To facilitate AC transmission between the coils, an IPT system also includes power electronic parts to transform direct current (DC) to AC at the primary side and to convert AC back to DC at the secondary. Of course, all the constituent parts affect the system performance, but the coil system is a dominant factor; and, improving the characteristics of the coils contributes to the performance enhancements. An important aspect of the coils is their quality factors (Q factors) as the power transfer efficiency (PTE) increases monotonically with these quantities. [3]–[5]. Another important aspect is the inductances. A coil system with larger inductances induces a larger output voltage for a given input current at a given transmission distance. If the mutual induatnces are too small, input current should be increased largely to achieve the same output voltage at the load. Achieving target output voltage without excessively raising the input current requires sufficiently large inductances. For that reason, this paper improves both the Q factor and the inductance for IPT coils. We focus our study on IP coils operating in MHz frequency range [6], especially the industrial, scientific and medical (ISM) frequencies of 6.78 MHz and 13.56 MHz because they are compact, low-cost, suitable for portable devices, and can be used widely without license.

IPT coils in the MHz frequency range are subject to many types of harmful effects, especially proximity effect and eddy current. To avoid losses, coils in this frequency range are usually small, single-strand, air-cored and loosely wound spiral form [7]. They have much smaller inductances compared to the coils operating in lower frequency range (for instance, the kHz range). Increasing the number of winding layers in a coil is an effective way to increase the inductances. Multi-layer coils, especially double-layer coils (DLCs) have been extensively investigated in the open literatures. Research efforts so far have focused mainly on the open-ended DLC [8]–[21] in which the layers are not connected together. The purpose is to increase the parasitic capacitance between the layers and realize self-resonance without adding external capacitors. This type of DLC has an advantage that it avoids losses in external capacitor and can achieve high Q factor. Another advantage is that it can avoid excessive voltage burden on external capacitors which would change the capacitances and detune the system [13], [19]. However, there is a little-known fact that the open-ended type is indeed contradict with the original motivation of DLCs. This type of DLCs sacrifices the inductance increasing effect since it utilizes the coil as a capacitor rather than as an inductor. On the contrary, series-connected DLCs [22], [23] where the layers are connected in series fully obtains the inductance increasing effect. A series-connected DLC has a disadvantage that it requires external capacitors for resonance which may introduce more losses and deteriorate the Q factor. If the Q factor of series-connected configuration is improved by some means, this type of DLCs is more suitable for many compact IPT applications installed into small devices. For that reason, this paper focuses on the series-connected DLCs and investigates a resonance scheme to improve the Q factor. The contributions of this paper are summarized below.

[†]The author is with the Faculty of Information Science and Technology, Osaka Institute of Technology, 1-79-1 Kitayama, Hirakata, Osaka 573-0196, Japan.

[††]The author is with the Artificial Intelligence Department, FPT University, Da Nang Campus, Ngu Hanh Son, Da Nang, Vietnam.

[†††]The author is with the Graduate School of Information Science, Nara Institute of Science and Technology, 8916-5 Takayama-cho, Ikoma, Nara 630-0192, Japan.

a) E-mail: duong.quang.thang@oit.ac.jp

- First, by using a lumped-element model derived from transmission line concept, this paper shows that the self inductance when the layers are serially connected is approximately 3 times of that when they are open-ended. This analytical result confirms the advantage of series-connected configuration over the open-ended configuration and motivates this research.
- Next, in order to improve Q factor for the series-connected configuration, this paper investigates a distributed resonance scheme using two capacitors: one inserted between the layers and the other added outside the coil. In the MHz frequency range, the operation frequency becomes comparable to the resonant frequency of the coil. In such a case, inserting tuning capacitors in the middle of the windings is an effective method to reduce dielectric loss and increase the efficiency [24], [25]. The loss reduction aspect has been investigated in the literatures. In this work, we study this method considering both the Q factor and the reactance aspects. In addition to confirming the Q enhancement effect [26], [27], our analysis shows a side effect that this method decreases the reactance when used in an IPT system. Based on a theoretical model, the capacitance is chosen to achieve sufficient Q enhancement while keeping the reactance from deteriorating too much.
- Experiments with air-cored coils having diameter of 100 mm and thickness of 3 mm are given to support the analytical results. The results show that the distributed tuning scheme increases the Q factor at 6.78 MHz from 242 to 308 while achieving an inductance of 7.69 µH. At the transmission distance of half of the diameter, our coils reach a maximum PTE of 94%, which gives enough margins for achieving the popular target 85% end-to-end (DC-to-DC) efficiency. Although the proposed design has an disadvantage of using two external capacitors, it has larger inductance and almost same Q factor with recently reported self-resonant coils having similar dimensions.

The remainder of this paper is organized as follows. Section 2 theoretically analyses the inductance enhancing effect of series-connected DLC, Q factor and maximum PTE of this configuration in the MHz frequency range. Section 3 analyzes the effect of distributed tuning capacitors. Section 4 provides full-wave simulation and experimental results in comparison with recent self-resonant open-ended DLCs. Finally, section 5 concludes this work.

2. Analysis based on lumped-element model

2.1 Reactance comparison with open-ended DLC

This paper focuses on the series-connected DLC illustrated in the left-hand side of Fig. 1. The coil has two layers, which are planar spiral windings connected in series to enhance the self inductance. Each layer is made of single wire and loosely wounded to avoid the proximity effect and eddy

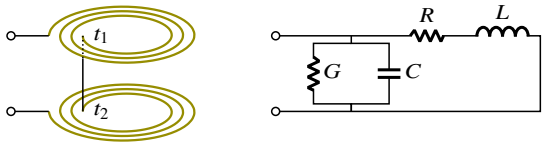

Fig. 1 Series-connected DLC. Winding directions of two layers are idential to achieve an enhanced self inductance. Spacing between layers are exaggerated for illustrative purposes. Intrinsic parameters R, L, G and C are assumed to be frequency-independent around the operating frequency.

current. The winding directions of the layers are kept identical; they are simultaneously clockwise or simultaneously counter-clockwise so that the mutual inductance between the layers adds constructively to the self inductance of the whole coil. The windings are usually placed on substrates but they are not shown in the figure for simplicity. In the figure, the spacing between the two layers is also exaggerated for illustrative purposes. In practice, this spacing is usually very small to facilitate the integrating into compact devices.

Since the phase shift of signal propagating in the coil is considerable, the trasmission line concept in [28], [29] can be used to model the series-connected DLC. In this model, the coil is seen as a short-circuited transmission line having characteristic impedance Z_0, complex propagation constant γ and length l. In more detail, Z_0 and γ can be expressed

$$Z_0 = \sqrt{\frac{R_0+j\omega L_0}{G_0+j\omega C_0}}, \gamma = \sqrt{(R_0+j\omega L_0)(G_0+j\omega C_0)} \quad (1)$$

where R_0 is the series resistance per unit length measured in Ω/m, L_0 is the series inductance per unit length in H/m, G_0 is the shunt conductance per unit length in S/m, C_0 is the shunt capacitance per unit length in F/m, and ω is the angular frequency of the signal. These parameters are the primary line constants of the transmission line model. Strictly speaking, the coil is a non-uniform line whose primary line constants may vary along the length l. However, as the total length is just a small portion of a wavelength, on average same values of R_0, L_0, G_0 and C_0 can be used for modeling signal at every point along the wire.

From transmission line theory [29], the admittance of the series-connected DLC is

$$\begin{aligned} Y = \frac{\coth(\gamma l)}{Z_0} &\approx \frac{1}{Z_0}\cdot\frac{1+\frac{1}{2}(\gamma l)^2}{\gamma l+\frac{1}{6}(\gamma l)^3} \\ &\approx \frac{1}{Z_0}\cdot\left(\frac{1}{\gamma l}+\frac{\gamma l}{3}\right) \\ &\approx \frac{1}{R_0 l+j\omega L_0 l}+\frac{G_0 l+j\omega C_0 l}{3} \end{aligned} \quad (2)$$

By letting $R = R_0 l$, $L = L_0 l$, $G = G_0 l/3$ and $C = C_0 l/3$, the admittance Y can be simplified

$$Y \approx \frac{1}{R+j\omega L}+G+j\omega C \quad (3)$$

The equivalent circuit is shown in the right-hand side

of Fig. 1. The series resistance R and the shunt conductor G represent conductor loss and dielectric loss, respectively. L represents the inductance of the whole coil, including the self inductance of the two layers and their mutual inductance. C represents all parasitic capacitances inside the coil. As the windings are loose, capacitance inside each layer is probably small and C mainly indicates the parasitic capacitance between the layers. Here, R, L, G and C are intrinsic parameters determined by the coil's shape, dimensions, number of turns, spacing between adjacent turns, spacing between two layers, substrate materials, etc. The intrinsic parameters are assumed to be frequency-independent for a narrow frequency range around the operating frequency (e.g., 6.78 MHz, 13.56 MHz).

The open-ended DLC with the same windings is obtained by removing the connection between terminals t_1 and t_2 in Fig. 1. This DLC type is shown in the left-hand side of Fig. 2. The open-ended version is the same transmission line (same characteristic impedance Z_0, complex propagation constant γ, length l) but terminated in an open-circuit [10]. Its input impedance is therefore

$$\begin{aligned} Z_{\text{open}} &= Z_0 \coth(\gamma l) \\ &\approx Z_0 \left(\frac{1}{\gamma l} + \frac{\gamma l}{3} \right) \\ &\approx \frac{R_0 l + j\omega L_0 l}{3} + \frac{1}{G_0 l + j\omega C_0 l} \\ &\approx \frac{R + j\omega L}{3} + \frac{1}{3G + j\omega 3C} \end{aligned} \tag{4}$$

As a result, the open-ended DLC can be modeled by the equivalent circuit illustrated in the right-hand side of Fig. 2. From (4), the input impedance of the open-ended DLC can also be approximated as

$$Z_{\text{open}} \approx \frac{1}{3} \left(R + \frac{G}{\omega^2 C^2} \right) + j \left(\frac{\omega L}{3} - \frac{1}{3\omega C} \right) \tag{5}$$

Equation (5) indicates that by adjusting the winding configurations, e.g., number of turns, spacing between adjacent turns, spacing between layers such that $\omega^2 LC = 1$, one can achieve self-resonance with the open-ended DLC. Such efforts have been performed extensively in literature.

The equivalent circuit in Fig. 2 is similar to popular model of a capacitor [28], implying that the open-ended DLC is in fact a capacitor, thus an enhanced inductance should not be expected. To be specific, the inductance parameter is reduced from L in the series-connected DLC to $L/3$ in the open-ended DLC, meaning that the mutual reactance will be reduced significantly when the open-ended DLCs are used. This advantage of the series-connected DLC helps it achieve the same target output voltage as the open-ended DLC with a much smaller input current and avoid the excessive input current during the charging process.

It is worth noting that the increase in the mutual reatance of the series-connected DLC system does not necessarily bring about an efficiency improvement as the internal resistance also increase by 3 times compared to the open-ended DLC scenario.

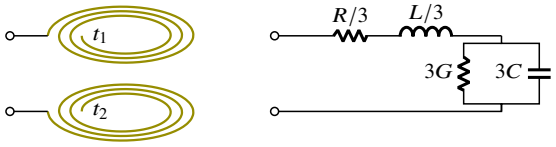

Fig. 2 Open-ended DLC with the same winding as the series-connected DLC in Fig. 1. Intrinsic parameters R, L, G and C are identical to those in Fig. 1.

The lumped-element model of the series-connected DLC in Fig. 1 also exhibits a parallel connection of the inductor L and the capacitor C. This fact implies that self-resonance is impossible in this design, and external capacitors are required to achieve resonance. Adding external capacitors introduces more losses and may deteriorate the Q factor of the coil but if the Q factor is improved by some means, the series-connected DLC is more suitable for many compact IPT applications installed into small devices.

2.2 Q factor

Hereafter, we focus our analysis on the series-connected DLC. From the lumped-element model in Fig. 1, the input impedance of the series-connected DLC is given by

$$Z = Y^{-1} = \left(\frac{1}{R + j\omega L} + G + j\omega C \right)^{-1} \tag{6}$$

Since IPT coils are usually low-loss and the considered frequency range (1–20 MHz) is quite high, it is reasonable to assume that $R \ll \omega L$ and $G \ll \omega C$. Due to space constraints the total conductor length of the coils is a small fraction of the signal wavelength. The term $\omega^2 LC$, which reflects the phase shift, can be assumed a fraction of one. Using the formula $(x + jy)^{-1} \approx x/y^2 - j/y$ for $x \ll y$ the input impedance therefore can be approximated as follows.

$$\begin{aligned} Z &\approx \left[\left(\frac{R}{\omega^2 L^2} + G \right) + j \left(\omega C - \frac{1}{\omega L} \right) \right]^{-1} \\ &\approx \frac{\left(\frac{R}{\omega^2 L^2} + G \right)}{\left(\omega C - \frac{1}{\omega L} \right)^2} - \frac{j}{\left(\omega C - \frac{1}{\omega L} \right)} \\ &\approx \frac{R + \omega^2 L^2 G}{(1 - \omega^2 LC)^2} + \frac{j\omega L}{1 - \omega^2 LC} \end{aligned} \tag{7}$$

In (7), the input impedance Z includes the resistive component R_1 and the inductive reactance X_1.

$$R_1 = \text{Re(Z)} = \frac{\text{R} + \omega^2 \text{L}^2 \text{G}}{(1 - \omega^2 \text{LC})^2} \tag{8}$$

$$X_1 = \text{Im(Z)} = \frac{\omega \text{L}}{1 - \omega^2 \text{LC}} \tag{9}$$

Conventionally, an external tuning capacitor is connected in series with the coil to cancel the inductive reactance X_1 in (7). Here, for simplicity we ignore the external capacitor in the equivalent circuit. The Q factor of the coil in the conventional resonance scheme is given by

$$Q = \frac{X_1}{R_1} = \frac{\omega L(1-\omega^2 LC)}{R+\omega^2 L^2 G} \tag{10}$$

In the kHz frequency range, the terms $\omega^2 LC$ and $\omega^2 L^2 G$ in (10) are negligibly small, $R_1 \approx R$, $L_1 \approx L$ and $Q \approx \omega L/R$. In the 1–20 MHz range, $\omega^2 LC$ becomes a fraction of 1, $\omega^2 L^2 G$ becomes a fraction of R. In this regime, the self inductance increases but the internal resistance increases faster, making the Q factor deteriorate from $\omega L/R$.

2.3 Maximum PTE

Fig. 3 illustrates an IPT system using two identical series-connected DLCs. The system is briefly illustrated on the left-hand side focusing only the coupled coils and ommiting the power electronic blocks as well as compensation networks. In each coil, the two layers are connected in series. The terminal pair of the coil at bottom forms port 1 and that of the coil on top forms port 2. V_{21} is the voltage induced in port 2 when the current at port 1 is I_1. Theoretical model is shown on the right-hand side. Here, M denotes the mutual inductance between only the two intrinsic inductances L. V'_{21} is the voltage induced in the intrinsic inductance of port 2 when the current in the intrinsic inductance of port 1 is I'_1. The value of M is assumed frequency-independent and is decided by the transmission distance as well as the orientation between the two coils.

The relation between the currents I_1 and I'_1 is

$$I'_1 = \frac{1}{(R+j\omega L)(G+j\omega C)+1} I_1 \tag{11}$$

The current I'_1 induces the voltage $V'_{21} = j\omega M I'_1$ in the intrinsic inductance of the secondary coil, resulting in the voltage V_{21} observed at port 2.

$$V_{21} = \frac{1}{(R+j\omega L)(G+j\omega C)+1} V'_{21} \tag{12}$$

Therefore, the mutual reactance X_{21} between the two coils is

$$X_{21} = \left|\frac{V_{21}}{I_1}\right| \approx \frac{\omega M}{(1-\omega^2 LC)^2}. \tag{13}$$

In lower frequency range, $\omega^2 LC \approx 0$, therefore the mutual reactance X_{21} can be seen to increase linearly with ω. In the MHz range, $\omega^2 LC$ is comparable to one, making X_{21} increases at a faster rate than the linear model.

The overall efficiency (DC-DC efficiency) of an IPT system is the multiplication of the DC-AC conversion efficiency at the primary side, PTE (AC-AC efficiency) between the coils, and the AC-DC conversion efficiency at the secondary. The overall efficiency is upper bounded by the PTE,

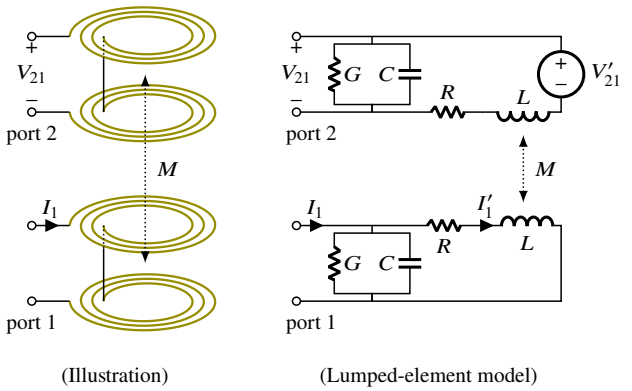

Fig. 3 IPT system using two identical series-connected DLCs. Illustration on the left-hand side shows only the RF part and ommits the DC-to-AC and the AC-to-DC power conversion blocks. V_{21} is induced voltage at port 2 when a current I_1 is input in port 1. Theoretical model on the right-hand side shows detail interaction between intrinsic inductances L.

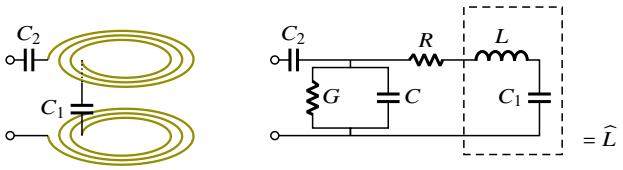

Fig. 4 Resonance for series-connected DLC with distributed capacitors C_1 and C_2. C_1 is inserted inside the coil between the two layers, and C_2 is added outside.

which is in its turn dominated by the kQ product [4], [5] of the pair of coils. The kQ product of an IPT system is given by the ratio of the square of mutual reactance to the product of the internal resistances of the coils. The kQ product of the considered IPT system in Fig. 3 is given by

$$(kQ)^2 = \frac{X_{21}^2}{R_1 \cdot R_1} = \left(\frac{\omega M}{R+\omega^2 L^2 G}\right)^2. \tag{14}$$

Although the PTE depends on both the kQ product and the load resistance, it is no doubt that a higher the kQ-product also means a higher PTE regardless of the load resistance. The kQ-product is the ultimate indicator of the efficiency but it is not intuitive, therefore the maximum PTE [3] is usually used instead. The maximum PTE is calculated directly from the kQ product following the formula below

$$\eta_{\max} = 1 - \frac{2}{1+\sqrt{1+(kQ)^2}} \tag{15}$$

$\eta_{\max}$ is a monotonically increasing function of the kQ product. The term $\omega^2 L^2 G$ reduces the kQ product according to (14), thus also reduces the maximum efficiency $\eta_{\max}$.

3. Resonance with distributed capacitors

The resonance scheme by two distributed tuning capacitors C_1 and C_2 for the series-connected DLC is illustrated in Fig. 4. The capacitor C_1 is inserted between the two layers,

and the capacitor C_2 is connected outside the coil. The input impedance of the coil including the two capacitors in this distributive resonance is given by

$$Z_{\text{distC}} = \left[\frac{1}{R+j\left(\omega L-\frac{1}{\omega C_1}\right)}+G+j\omega C\right]^{-1}-\frac{j}{\omega C_2} \quad (16)$$

An approximation of the first term of (16) can be obtained by replacing ωL in (7) by $\omega L - \frac{1}{\omega C_1}$, thus Z_{distC} can be approximated as follows.

$$\begin{aligned} Z_{\text{distC}} &\approx \frac{R+G(\omega L-\frac{1}{\omega C_1})^2}{(1+C/C_1-\omega^2 LC)^2}+\frac{j\omega L-\frac{j}{\omega C_1}}{1+C/C_1-\omega^2 LC}-\frac{j}{\omega C_2} \\ &\approx \frac{R+G(\omega L-\frac{1}{\omega C_1})^2}{(1+C/C_1-\omega^2 LC)^2}+\frac{j\omega L}{1+C/C_1-\omega^2 LC} \\ &\quad -\left(\frac{1}{1+C/C_1-\omega^2 LC}\cdot\frac{j}{\omega C_1}+\frac{j}{\omega C_2}\right) \end{aligned} \quad (17)$$

In (17), the first term is the resistive component, the second term is the inductive rectance and the third term is the capacitive reactance. At resonance, the inductive reactance balances with the capacitive reactance. To this end, the value of C_2 is determined accordingly to the value of C_1

$$C_2 = \frac{1+C/C_1-\omega^2 LC}{\omega^2 L-1/C_1} \quad (18)$$

The resistive component and the inductive reactance are

$$R_{1-\text{distC}} = \frac{R+G(\omega L-\frac{1}{\omega C_1})^2}{(1+C/C_1-\omega^2 LC)^2} \quad (19)$$

$$X_{1-\text{distC}} = \frac{\omega L}{1+C/C_1-\omega^2 LC} \quad (20)$$

Equation (19) indicates that inserting C_1 reduces the impact of dielectric loss G and conductor loss R. This effect has been discussed in [24], [25] and it is reconfirmed here by our theoretical analysis. Importantly, (20) shows another effect of inserting C_1 that it also reduces the inductive reactance. This side effect has not been mentioned in previous studies. The decrease in the self reatance $X_{1-\text{distC}}$ will not yield a decrease in Q factor as the resistive component $X_{1-\text{distC}}$ decreases faster with C_1. However, it will reduces the mutual reatance when the coil is used in an IPT system.

The Q factor is the ratio of the inductive rectance to the resistive component

$$Q_{\text{distC}} = \frac{X_{1-\text{distC}}}{R_{1-\text{distC}}} = \frac{\omega L(1+C/C_1-\omega^2 LC)}{R+G(\omega L-\frac{1}{\omega C_1})^2}. \quad (21)$$

It is obvious that Q_{distC} in (21) is larger than Q in (10) for the conventional resonance scheme. The Q ratio between the distributive resonance and the conventional resonance is

$$\frac{Q_{\text{distC}}}{Q} = \frac{(1+C/C_1-\omega^2 LC)(R+\omega^2 L^2 G)}{(1-\omega^2 LC)[R+G(\omega L-\frac{1}{\omega C_1})^2]} \geq 1 \quad (22)$$

When two identical DLCs with distributive resosnance scheme are used in an IPT system, the mutual reactance can be straightforwardly obtained from (13) by replacing ωL with $\omega L - \frac{1}{\omega C_1}$.

$$X_{21-\text{distC}} = \frac{\omega M}{(1+C/C_1-\omega^2 LC)^2} \quad (23)$$

The mutual reactance $X_{21-\text{distC}}$ is smaller than the mutual reactance X_{21} in (13) for conventional resonance with one capacitor. The mutual reactance ratio is

$$\frac{X_{21-\text{distC}}}{X_{21}} = \left(\frac{1-\omega^2 LC}{1+C/C_1-\omega^2 LC}\right)^2 \leq 1 \quad (24)$$

Similarly, the kQ product of this IPT system is

$$(kQ)^2_{\text{distC}} = \frac{X^2_{21-\text{distC}}}{R^2_{1-\text{distC}}} = \left[\frac{\omega M}{R+G(\omega L-\frac{1}{\omega C_1})^2}\right]^2 \quad (25)$$

which is larger than the kQ product in (14) for conventional resonance scheme. The kQ product ratio is

$$\frac{(kQ)^2_{\text{distC}}}{(kQ)^2} = \left[\frac{R+\omega^2 L^2 G}{R+G(\omega L-\frac{1}{\omega C_1})^2}\right]^2 \geq 1 \quad (26)$$

In summary, inserting C_1 reduces the mutual reactance but increases the Q factors and the kQ product. Using a smaller C_1 yields higher Q and efficiency but it also brings about a smaller mutual reactance. Both Q factor and the reactance are important aspects of the coupling link, therefore C_1 should be flexibly decided accordingly to the design target (C_2 is not so important as it will be determined accordingly to C_1 to cancel out the remaining reactance.) The ratios of Q, kQ and mutual reactance for a given C_1 can be predited from (22), (26), (24) and the parameters R, L, G, C.

4. Computer simulation and experimental results

4.1 Reactance enhancing effect of series-connected DLC

Fig. 5 shows setup and results of a full-wave electromagnetic (EM) simulation to measure the mutual inductance of an IPT system using two identical uniform double-layer coils. In this simulation, each layer is a planar spiral winding having 6 turns, outer diameter of 100 mm, spacing between adjacent turns is set to 5 mm, 6 mm or 7 mm. The conductor is copper foil (conductivity: 58×10^6 S/m) with thickness of 0.1 mm and width of 2 mm. In each coil, the spacing between layers is 1 mm and the windings have the same direction to enhance the self inductance. The two coils are both series-connected DLCs or both open-ended DLCs. In each case, the two coils are placed coaxially in vacuum with varying transmission distance. For fast calculations, this simulation uses the method of moments (MoMs) provided by the commerial software WIPL-D Pro v17. The coils are connected to two ports having reference impedance of 50 Ω to calculate

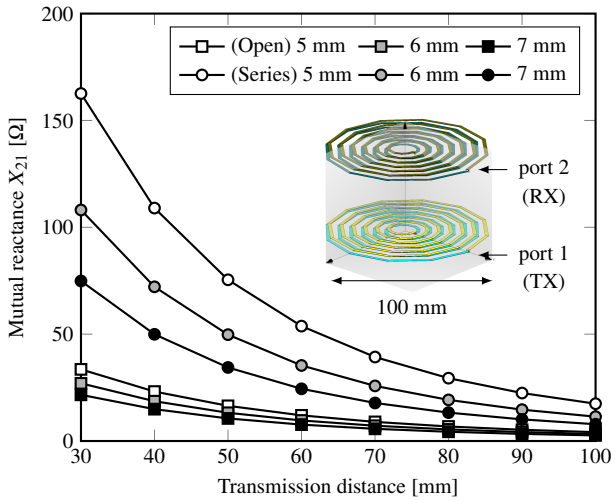

Fig. 5 Mutual reactance comparison of IPT using open-ended DLCs and IPT using series-connected DLCs by EM simulation.

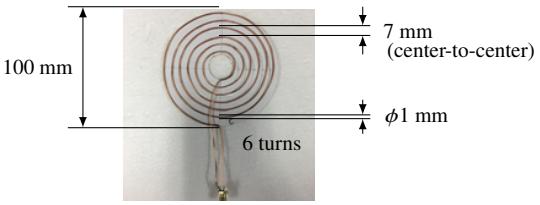

Fig. 6 Parameters of 1 layer planar spiral coil.

Table 1 Measurements of 1 layer spiral coil in Fig. (6)

Internal resistance	Inductance
418 mΩ	2.22 µH

Table 2 Parameter extraction results for double-layer coil.

R	L	G	C
444 mΩ	7.69 µH	5.88 µS	13.60 pF

the Z parameters. For the turn spacing of 5 mm, 6mm and 7 mm, the self impedance of the series-connected DLC is measured as 551 Ω, 405 Ω and 303 Ω respectively while these values for the open-ended DLC is -584 Ω, -714 Ω and -866 Ω, respectively. This simulation result indicates that the open-ended DLC behaves as a capacitor rather than as an inductor. Also, from the transimpedance parameter Z_{21}, mutual reactance between the coils $X_{21} = \mathrm{Im}(Z_{21})$ is extracted and plotted on the graph of Fig. 5. The graph shows that when the series-connected DLCs are employed, the mutual reactance is enhanced by approximately 3–5 times compared to that when the open-ended DLCs are used. These simulation results confirm the theoretical observation mentioned in section 2.1.

4.2 Sample coil fabrication

4.2.1 Extraction of intrinsic parameters

Now, we perform experimental evaluations on series-connected DLC with distributive resonance scheme. In order to frabricate sample coils following performance prediction mentioned in section 3, we extract intrinsic parameters R, L, G and C in the lumped-element model. First, we measure one single-layer coil shown in Fig.6. The single-layer coil is a planar spiral winding of $N = 6$ turns, with outer diameter of 100 mm and 7 mm spacing between adjacent turns. Considering the skin effect, IPT coils in the MHz frequency range should be made of thin metal foil to save conductor material volume. However, as the main purpose here is to evaluate performance of the distributive resonance scheme instead of focusing on detail configurations of the coils, we use small cylindrical wire for ease of fabrication. The winding is made of copper wire with a diameter of 1 mm and is placed on a plastic substrate with a thickness of 0.5 mm. The mean radius of the windings is $a = 0.032$ m and the thickness of the windings is $c = 0.036$ m. The coil is loosely wounded and the conductor length is about 1 m which is quite short compared to the wavelength of signals in the frequency range of interest. Thus, this coil can be represented by a series circuit of an internal resistor and an inductor. Fitting this linear model to the input impedance measured over the frequency range 6.58–6.98 MHz (6.78 ± 0.2 MHz), we obtained an internal resistance of 418 mΩ and self-inductance of 2.22 µH as in Tab. 1. Substituting parameters N, a and c of the coil into the formula in [30] results a theoretical value of its sell-inductance

$$L_{1\mathrm{layer-theo}} = 31.33\,\mu_0\,N^2\frac{a^2}{8a+11c} \approx 2.23\ [\mathrm{H}] \qquad (27)$$

where $\mu_0 = 4\pi \times 10^{-7}$ H/m is the magnetic permeability of free space. The theoretical result of self-inductance is close to the measurement.

Next, we extract intrinsic parameters for a series-connected DLC. Each layer of the coil has similar configuration with the spiral coil in Fig. 6. The winding directions of the two layers are kept identical (clockwise or counter-clockwise) so that their mutual inductance adds constructively to the self-inductance of the whole coil. In this case, the coil is modeled by the equivalent circuit introduced in Section 2 instead of the simple linear model due to the longer conductor and larger parasitic capacitance. To extract parameters for the model, we employ linearization technique introduced in [28]. From (6), the input impedance of the coil can be approximated as

$$Y \approx \left(\frac{R}{\omega^2 L^2} + G\right) + j\left(\omega C - \frac{1}{\omega L}\right) \qquad (28)$$

The parameters R, L, G, and C can be extracted by breaking (28) into real component and imaginary component.

$$\mathrm{Re}(Y) \approx \frac{R}{L^2}\cdot\frac{1}{\omega^2} + G \qquad (29)$$

$$\frac{\mathrm{Im(Y)}}{\omega} \approx -\frac{1}{L}\cdot\frac{1}{\omega^2} + C \qquad (30)$$

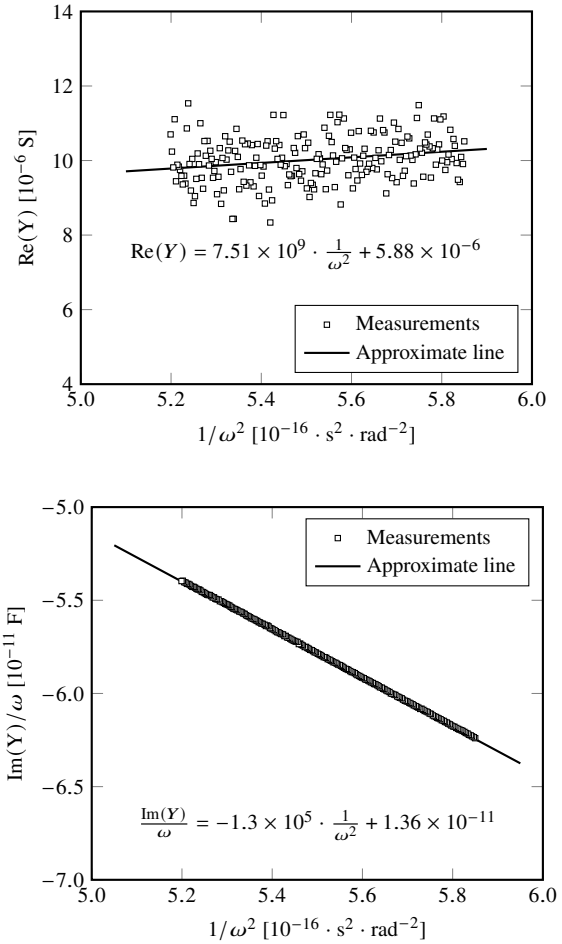

Fig. 7 Parameter extraction for series-connected DLC. Top figure: y-intercept and gradient of Re(Y) shows G and R/L^2. Bottom figure: y-intercept and gradient of Im(Y)/ω shows C and $-1/L$.

(29) and (30) can be plotted as two linear functions of $1/\omega^2$. The y-intercept and the gradient of (29) shows the value of G and R/L^2, respectively. Similarly, the y-intercept and the gradient of (30) indicate C and $-1/L$, respectively. Measuring admittance of the double-layer coil over the frequency range of 6.58–6.98 MHz (6.78 ± 0.2 MHz), we plot the approximate lines for (29) and (30) in Fig. 7. Intrinsic parameters R, L, G and C are then drawn and shown in Tab. 2. L is about 3.5 times of the self inductance of one layer. This value is understandable since the two layers are close to each other and their mutual inductance probably accounts for 75% of the self inductance of each layer.

4.2.2 Sample coils

Three sample coils for experimental evaluations are described in Fig. 8. Here, coil 1 has similar configurations with the single-layer coil in Section 4.2.1 and is resonated by an external capacitor of 267 pF. Coil 2 has similar configurations with the double-layer coil in Section 4.2.1 and is resonated by an external capacitor of 59 pF. Coil 3 has similar layer configurations with coil 2, except that it is resonated by

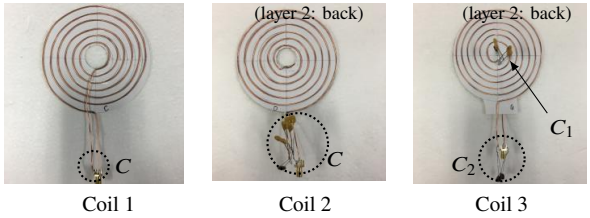

Fig. 8 Three types of spiral coils with tuning capacitors. Coil 1: single-layer coil with 1 capacitor C = 267.0 pF. Coil 2: double-layer coil with 1 capacitor C = 59 pF. Coil 3: double-layer coil with 2 capacitors C_1 = 267.0 pF and C_2 = 88.6 pF.

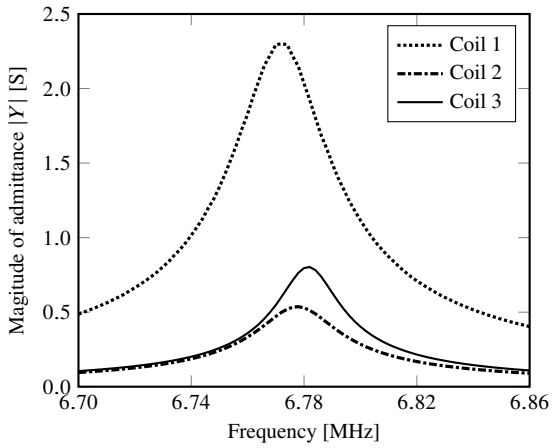

Fig. 9 Q factor measurement by bandwidth method for three coils in Fig. 8. Resonant frequencies are respectively 6.772 MHz, 6.778 MHz and 6.782 MHz, quite close to the target 6.78 MHz.

Table 3 Estimates and measurements of Q factor

	Estimates (no capacitors)	Measurements (capacitors added)
Q factor of Coil 1	227	225
Q factor of Coil 2	247	242
Q factor of Coil 3	361	308

two distributed capacitors: C_1 = 267 pF placed between the two layers and C_2 = 88.6 pF placed outside. The value of C_1 is chosen to significantly enhance the kQ product but does not deteriorate the mutual inductance so much. The value of C_2 is chosen to cancel out all the residual self inductance. At the frequency of 6.78 MHz, C_1 yields a negative reactance that cancels 26.8% of the intrinsic inductance L. Substituting the parameters R, L, G, C into (22), (24) and (26) we can predict that coil 3 system has a mutual indctance of 0.89 times, a Q of 1.46 times and a kQ of 1.89 times of those of coil 2. Therefore, it is expected that the coil 3 system has a significantly enhanced efficiency and maintains a nearly similar mutual inductace with the coil 2 system.

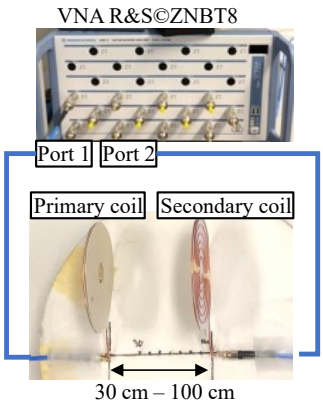

Fig. 10 Experimental setup.

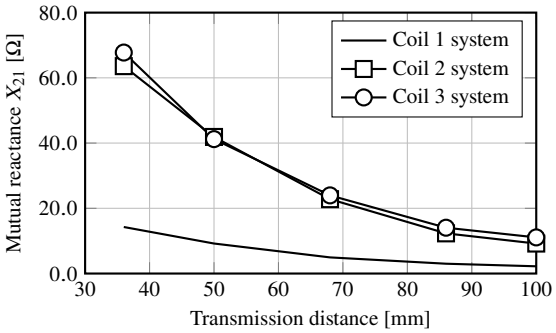

Fig. 11 Measurements of mutual reactance

4.3 Q factor

Q factor measurements by bandwidth method are demonstrated in Fig. 9. The resonant frequencies of coil 1 is 6.772 MHz, coil 2 is 6.778 MHz, and coil 3 is 6.782 MHz, which are quite close to the target frequency of 6.78 MHz. Tab. 3 compares the measured Q factors by bandwidth method and the estimations based on the theoretical models with intrinsic parameters extracted in Sect. 4.2.1. The estimate $Q = 227$ for coil 1 (single-layer coil) is based on the linear model with parameters given in Tab. 1. This value is quite close to the measured result of 225. The estimate of Q for coil 2 (the double-layer coil with one tuning capacitor) is 247 obtained by substituting the parameters in Tab. 2 into (10). This estimate is also close to the measured Q of 242. The estimate for coil 3 (the double-layer coil with two tuning capacitors) is 361 obtained from substituting parameters in Tab. 2 and $C_1 = 267$ pF into (21). The measured Q factor in this case is 308, which is deteriorated from the estimate due to losses inside the capacitor C_1.

4.4 Maximum PTE

The three coils in Fig. 8 are replicated to construct three IPT systems below

- Coil 1 system: both the primary side and secondary side use the single-layer coil
- Coil 2 system: both the sides use the double-layer coil with one tuning capacitor
- Coil 3 system: both the sides use the double-layer coil with two tuning capacitors

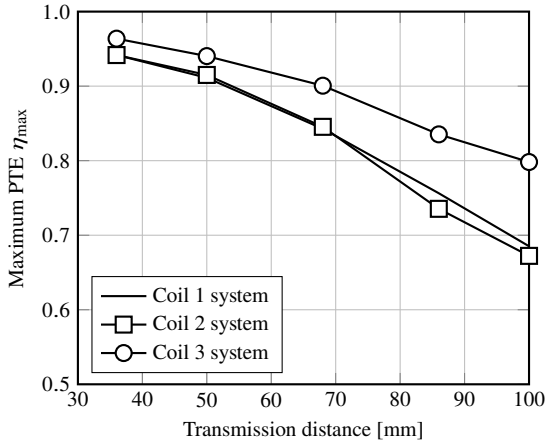

Fig. 12 Measurements of maximum PTE

The experimental setup is shown in Fig. 10. The input port and output port of each system are connected to vector network analyzer (VNA) R&S©ZNBT8 to measure the Z-parameters at 6.78 MHz for different transmission distance. The reference impedance of the VNA is 50 Ω.

Fig. 11 plots the measurements of mutual reactance $X_{21} = \mathrm{Im}(Z_{21})$. This figure indicates that the two systems using double-layer coils (the coil 2 system and the coil 3 system) have similar mutual reactances. This measured result is quite agrees with the theoretical estimation that the mutual reactance ratio is about 0.89. The mutual reactances of the two systems above are about 3.5 times of that of the system using single-layer coils (the coil 1 system). This result is supported by the measurements in Sect. 4.2.1, showing that the self-inductance of double-layer coil is approximately 3.5 times larger than that of the single-layer coil.

Fig. 12 depicts the maximum PTE calculated by (15) with the kQ product is calculated from the Z-parameters [4] as follows because the coils are placed in the air.

$$(kQ)^2 = \frac{|Z_{21}|^2}{\mathrm{Re}(Z_{11}) \cdot \mathrm{Re}(Z_{22})}. \tag{31}$$

The figure indicates that the system of double-layer coils with two tuning capacitors (coil 3 system) significantly outperforms the system of conventional double-layer coils (coil 2 system). The efficiency is enhanced in coil 3 because the distributed capacitor C_1 reduces the impact of dielectric loss represented by G in (26). This explanation agreees with detail analysis in [25]. Also, the single-layer coil system achieves similar efficiency with the system of double-layer coils with conventional resonance. This is because the two systems have similar Q factors and the coupling coefficients seem also similar as shown in Fig. 13.

When looking only at Q factor and PTE, it seems that

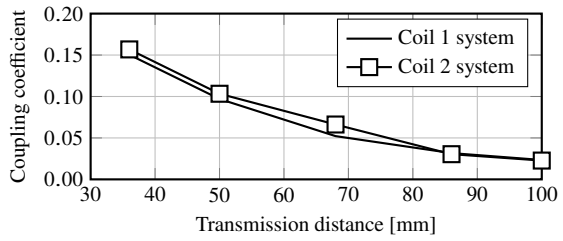

Fig. 13 Coupling coefficient comparision of coil 1 system and coil 2 system.

Table 4 Comparison with reported self-resonance coils

Ref.	f (MHz)	Diameter (mm)	Height (mm)	Q-factor	Inductance (μ H)
[12]	7	66	16	1183*	NA
[17]	3	400	2	452	5.2~6.7
[14]	6.78	100	~1	185	NA
[15]	6.47	100	1.5	220	NA
[19]	13.56	100	1~2.5	178	5.24
This work	6.78	100	3	308	7.69

*Note: [12] uses magnetic core (NA: Not Available)

there is no need for double-layering as coil 1 and coil 2 have similar performances. However, taking the mutual reactance into account, coil 2 becomes a better option as it significantly outperforms coil 1 in this aspect. Superior in both the Q factor and the reactannce aspects, the double-layer coil with two tunning capacitors is the best option after all.

4.5 Discussion

A comprehensive comparison between the proposed series-connected DLC and the state-of-the-art self-resonant coils is complicated and beyond the scope of this paper. However, a rough comparision can be carried out to further confirm the simulation results and experimental results achieved above. Q factors of state-of-the-art self-resonant coils are listed on Tab. 4. The highest Q of 1183 achieved in [12] with a multi-layer coil placed inside a magnetic core. The second highest Q of 452 belongs to the coil in [17], however this coil has a much larger outer diameter (four times) compared to that of the double-layer coil is this work. The aforementioned two coils have quite different dimensions and/or settings with this work but they are still listed in the table for reference. Prototypes having similar dimensions and operating frequencies can be found in [14], [15] and [19] with Q factors around 200. Meanwhile our coil achieves a higher Q of 308 even though it uses lossy external capacitors.

When used in an IPT system, our coil system reaches a maximum PTE of 94% at the transmission distance of 50 mm (half of the outer diameter). This provides enough margins to achieve a target DC-DC efficiency of 85% which is a popular criterion in IPT technology. The coils in [19] which have similar dimensions achieve a lower maximum PTE of about 90% at the same transmission distance.

From the comparisons above, it is no exaggeration to say that our sample series-connected DLCs exhibits a Q factor as good as if not better than that recently reported self-resonant open-ended DLCs.

As for the self inductance, our design achieves 7.69 µH, while the coils in [17] with the same number of turns (12 turns) but has an much larger (4 times) outer diameter exhibit smaller values of 5.2 µH and 6.7 µH for different conductor trace widths. Compared to our coil, the coil in [19] has similar dimensions and more turns (16 turns) but achieves a smaller inductance of 5.24 µH.

5. Conclusions

By comparing theoretical models of the open-ended DLC and the series-connected DLC, this paper has confirmed that the former can achieve capacitor-less self resonance while the latter cannot. More important, this paper has shown that the series-connected DLC can achieve a self inductance of approximately more than 3 times of that of the open-ended DLC. Motivated by this fact, this paper has focused on the series-connected design and investigated a resonance scheme using two tuning capacitors. In this paper, the capacitance inserted between the layers is chosen carefully to sufficiently enhance the Q factor and maintain the self inductance. However, in application this capacitance can be flexibly decided according to the target Q factor and inductance. Experiments with air-cored coils having diameter of 100 mm and frequency of 6.78 MHz show that the distributed tuning scheme increases the Q factor from 242 to 308 while almost maitaining the same mutual reactance. Compared with recently reported self-resonant coils, our design achieves larger inductance and a similar or even better Q factor although it has a disadvantage of using external lossy capacitors.

6. Acknowledgments

This work was supported in part by JSPS KAKENHI Grant Number 22K04087.

References

[1] G. A. Covic and J. T. Boys, "Inductive power transfer," *Proceedings of the IEEE*, vol. 101, no. 6, pp. 1276–1289, June 2013.
[2] N. Shinohara, "Trends in Wireless Power Transfer," *IEEE Microw. Mag.*, vol. 22, no. 1, pp. 46–59, Dec. 2020.
[3] M. Zargham and P. G. Gulak, "Maximum achievable efficiency in near-field coupled power-transfer systems," *IEEE Trans. Biomed. Circuits Syst.*, vol. 6, no. 3, pp. 228–245, June 2012.
[4] T. Ohira, "Maximum available efficiency formulation based on a black-box model of linear two-port power transfer systems," *IEICE Electron. Express*, vol. 11, no. 13, pp. 1–6, July 2014.
[5] T. Ohira, "Extended k-Q product formulas for capacitive- and inductive-coupling wireless power transfer schemes," *IEICE Electron. Express*, vol. 11, no. 9, pp. 1–7, Apr. 2014.
[6] Y. Akuzawa, Y. Ito, T. Ezoe, and K. Sakai, "A 99%-efficiency GaN converter for 6.78 MHz magnetic resonant wireless power transfer system," J. Eng., vol. 2014, no. 10, pp. 598–600, Oct. 2014.
[7] C.-C. Hou, W.-P. Chang, Y.-H. Teng and K.-J. Lee, "Planar spiral coils for inductive power transfer systems," in *Proc. IEEE 2nd Int. Future Energy Electron. Conf. (IFEEC)*, Nov. 2015, pp. 1–6.

[8] K. Chen and Z. Zhao, "Analysis of the Double-Layer Printed Spiral Coil for Wireless Power Transfer," *IEEE Trans. Emerg. Sel. Topics Power Electron.*, vol. 1, no. 2, pp. 114–121, June 2013.
[9] K. Furusato, T. Imura, and Y. Hori, "Improvement of 85 kHz Self-resonant Open End Coil for Capacitor-less Wireless Power Transfer System," 2016 Asian Wireless Power Transfer Workshop , pp. 1–4, Chengdu, China, Dec. 2016.
[10] K. Furusato, T. Imura, and Y. Hori, "Design of Multi-frequency Coil for Capacitor-less Wireless Power Transfer using High Order Self-resonance of Open End Coil," in *Proc. IEEE Wireless Power Transf. Conf.*, 2016, pp. 1–4.
[11] A. L. F. Stein, P. A. Kyaw and C. R. Sullivan, "High-Q self-resonant structure for wireless power transfer," in *Proc. IEEE Annu. Appl. Power Electron. Conf. (APEC)*, Mar. 2017, pp. 3723–3729.
[12] A. L. F. Stein, P. A. Kyaw and C. R. Sullivan, "Wireless Power Transfer Utilizing a High-Q Self-Resonant Structure," *IEEE Trans. Power Electron.*, vol. 34, no. 7, pp. 6722–6735, July 2019.
[13] C. M. de Miranda and S. F. Pichorim, "Alternative Configuration of Open-Bifilar Coil for Self-Resonant Wireless Power Transfer System," in *Proc. IEEE Wireless Power Transf. Conf.*, 2019, pp. 116–119.
[14] J. Li and D. Costinett, "Analysis and design of a series self-resonant coil for wireless power transfer," in *Proc. IEEE Annu. Appl. Power Electron. Conf. (APEC)*, 2018, pp. 1052–1059.
[15] R. Qin and D. Costinett, "Multi-layer Non-uniform Series Self-resonant Coil for Wireless Power Transfer," in *Proc. IEEE Energy Convers. Congr. Expo. (ECCE)*, 2019, pp. 3333–3339.
[16] Y. Park, J. Kim and K. Na, "Resistance and Q-factor calculation of single and double layer coils with split circular pattern," in *Proc. IEEE Wireless Power Transf. Conf.*, 2020, pp. 304–307.
[17] R. Qin, J. Li and D. Costinett, "A High Frequency Wireless Power Transfer System for Electric Vehicle Charging Using Multi-layer Nonuniform Self-resonant Coil at MHz," in *Proc. IEEE Energy Convers. Congr. Expo. (ECCE)*, 2020, pp. 5487–5494.
[18] R. Qin, J. Li and D. Costinett, "A 6.6-kW High-Frequency Wireless Power Transfer System for Electric Vehicle Charging Using Multi-layer Nonuniform Self-Resonant Coil at MHz," *IEEE Trans. Power Electron.*, vol. 37, no. 4, pp. 4842–4856, Apr. 2022.
[19] Z. Yi, M. Li, B. Muneer, G. He and X. -X. Yang, "Self-Resonant Antisymmetric Planar Coil for Compact Inductive Power Transfer System Avoiding Compensation Circuits," *IEEE Trans. on Power Electron.*, vol. 36, no. 5, pp. 5121–5134, May 2021.
[20] Q. Wang, M. A. Saket, A. Troy and M. Ordonez, "A Self-Compensated Planar Coil for Resonant Wireless Power Transfer Systems," *IEEE Trans. Power Electron.*, vol. 36, no. 1, pp. 674–682, Jan. 2021.
[21] Y. Mao, K. Wang, Y. Yang, "Double-Layer Coil Designs and Combined Current Flow Regulation Schemes for Octangle Wireless Charging Containers," in *Proc. 2022 IEEE Wireless Power Week (WPW)*, Bordeaux, France, 2022, pp. 433–437.
[22] H. Hirayama, T. Amano, N. Kikuma and K. Sakakibara, "A consideration of open- and short-end type helical antennas for magnetic-coupled resonant wireless power transfer," 2012 6th European Conference on Antennas and Propagation (EUCAP), 2012, pp. 3009-3013.
[23] Z. Li, X. He, Z. Shu, "Design of coils on printed circuit board for inductive power transfer system," *IET Power Electron.*, vol. 11, no. 15, pp. 2515–2522, Nov. 2018.
[24] S. C. Tang, "A Low-Operating-Voltage Wireless Intermediate-Range Scheme for Energy and Signal Transmission by Magnetic Coupling for Implantable Devices," *IEEE J. Emerg. Sel. Top. Power Electron.*, vol. 3, no. 1, pp. 242–251, Mar. 2015. IEEE J. Sel. Top. Quantum Electron.
[25] S. C. Tang and N. J. McDannold, "Power Loss Analysis and Comparison of Segmented and Unsegmented Energy Coupling Coils for Wireless Energy Transfer," *IEEE J. Emerg. Sel. Top. Power Electron.*, vol. 3, no. 1, pp. 215–225, Mar. 2015.
[26] S.-H. Lee and K.-P. Yi, "Development of 50W High Quality Factor Printed Circuit Board Coils for a 6.78MHz, 60cm Air-gap Wireless Power Transfer System," *J. Korean Soc. Railw.*, vol. 19, no. 4, pp. 468–479, Aug. 2016.
[27] S.-H. Lee, K.-P. Yi, and M.-Y. Kim, "6.78-MHz, 50-W Wireless Power Supply Over a 60-cm Distance Using a GaN-Based Full-Bridge Inverter," *Energies*, vol. 12, no. 3, pp. 371–391, Jan. 2019.
[28] K. Lee, S. Mohammadi, P. K. Bhattacharya and L. P. B. Katehi, "Compact Models Based on Transmission-Line Concept for Integrated Capacitors and Inductors," *IEEE Trans. Microw. Theory Techn.*, vol. 54, no. 12, pp. 4141–4148, Dec. 2006.
[29] D. M. Pozar, *Microwave Engineering*, 4th ed. John Wiley & Sons, Nov. 2011.
[30] H. A. Wheeler, "Simple Inductance Formulas for Radio Coils," *Proceedings of the IRE*, vol. 16, no. 10, pp. 1398–1400, Oct. 1928.

Quang-Thang Duong received the B.E., M.E., and Ph.D. degrees in communications engineering from Osaka University, Osaka, Japan, in 2009, 2011, and 2014, respectively. In 2014, he joined Nara Institute of Science and Technology as a Postdoctoral research assistant and then became an Assistant Professor in 2016. In 2023, he joined Osaka Institute of Technology as an Associate Professor. His research interests include broadband wireless access techniques, channel estimation, information theory, error correcting code, wireless power transfer, and simultaneous wireless information and power transfer. He is a member of the Institute of Electrical, Information and Communication Engineers (IEICE) and the Institute of Electrical and Electronics Engineers (IEEE). He is the recipient of the Young Engineer Award and the Michiyuki Uenohara Memorial Award from the IEEE Microwave Theory and Techniques Society (IEEE-MTTS) Japan Chapter in 2019.

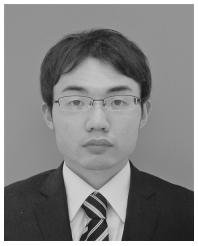

Kohei Matsukawa received the B.E. degree in electrical engineering from the KINDAI University, Osaka, Japan in 2020 and the M.E. degree in Information Science from Nara Institute of Science and Technology, Nara, Japan in 2022. His current research interests include wireless power transfer technique.

Quoc-Trinh Vo received the B.E. degree in electronics-telecommunications engineering from Da Nang University of Science and Technology, Viet Nam, in 2010, the M.E in electronics engineering from International University, Vietnam National University, Ho Chi Minh City, Viet Nam, in 2013, and the D.Eng. from Nara Institute of Science and Technology, Nara, Japan, in 2021. In 2022, he joined FPT University, Da Nang Campus, Viet Nam as a lecturer. His interests include wireless power transfer, wireless communication and digital signal processing.

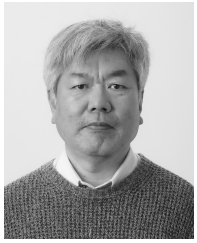

Minoru Okada received the B.E. degree in communications engineering from the University of Electro-Communications, Tokyo, Japan, in 1990, and the M.E. and Ph.D. degrees in communications engineering from Osaka University, Osaka, Japan, in 1992 and 1998, respectively. From 1993 to 2000, he was a Research Associate with Osaka University. From 1999 to 2000, he was a Visiting Research Fellow with the University of Southampton, Southampton, U.K. In 2000, he joined the Graduate School of Information Science, Nara Institute of Science and Technology, Ikoma, Japan, as an Associate Professor and then became a Professor. His current research interests include wireless communications, including WLAN, WiMAX, code division multiple access, OFDM, and satellite communications. Dr. Okada is a member of the Institute of Television Engineers of Japan, Institute of Electrical, Information, and Communication Engineers (IEICE), Japan, and the Information Processing Society Japan. He was the recipient of the Young Engineer Award from the IEICE in 1999.